

RESEARCH

Open Access



# Ironing out the conflicts: iron supplementation reduces negatives bacterial interactions in the rhizosphere of an Atacama-endemic perennial grass

Constanza Aguado-Norese<sup>1,2</sup>, Jonathan E. Maldonado<sup>3</sup>, Christian Hodar<sup>1,2</sup>, Gabriel Galvez<sup>1,2</sup>, Daniel E. Palma<sup>1,2</sup>, Verónica Cambiazo<sup>1,2</sup> and Mauricio Gonzalez<sup>1,2\*</sup>

## Abstract

**Background** In plants, root exudates selectively influence the growth of bacteria that colonize the rhizosphere. Bacterial communities associated with root systems are involved in macro and micronutrients cycling and organic matter transformation. In particular, iron is an essential micronutrient required for the proper functioning of iron-containing enzymes in processes such as photosynthesis, respiration, biomolecule synthesis, redox homeostasis, and cell growth in plants. However, the impact of changes of iron availability on the structure and set of ecological interactions taking place in the rhizosphere remains poorly understood. In this study, field experiments were conducted to compare the effects of iron supplementation (0.1 and 0.5 mM of FeSO<sub>4</sub>) on the assembly of the bacterial community of rhizosphere soil and bulk soil in a perennial grass present in the Andes steppe of Atacama Desert.

**Results** The results indicated that the difference in beta diversity between bulk soil and rhizosphere soil detected before supplementation did not persist after iron supplementation, in addition, co-occurrence networks showed a significant reduction in negative interactions among soil bacteria, mainly in rare taxa (< 0.1% relative abundance).

**Conclusions** These observations suggest that iron availability contributes to the differentiation between bulk soil and rhizosphere bacterial communities, a process that is linked to significant changes in the relative abundance of more abundant species (> 0.1% relative abundance) and with a decrease in the negative interactions in both compartments after metal exposure. The differential effect of iron on the competition/cooperation ratio between bulk soils and the rhizosphere microbiome supports the hypothesis that the host limits the degree of cooperation that can be achieved by the bacterial community associated with an organ dedicated to nutrient absorption.

**Keywords** Soil microbiota, Co-occurrence networks, Iron supplementation, Bacteria, Nutrients

\*Correspondence:  
Mauricio Gonzalez  
mgonzale@inta.uchile.cl

<sup>1</sup>Bioinformatic and Gene Expression Laboratory, INTA-Universidad de Chile, Santiago, Chile

<sup>2</sup>Millennium Institute Center for Genome Regulation, Santiago, Chile  
<sup>3</sup>Plant Multiomics and Bioinformatic Laboratory, Department of Biology, Faculty of Chemistry and Biology, Universidad de Santiago de Chile, Santiago, Chile



## Background

In natural environments, soil microorganisms form rich and complex assemblies of hundreds of species with diverse metabolic capabilities living in a common habitat [1, 2], where a few species are highly abundant and a large number of other species are in low abundance, referred to as the rare biosphere [3]. The structure (composition and abundance) of soil bacterial communities is influenced by environmental variables, such as soil pH [4, 5], relative humidity [6, 7], temperature [8], and nutrient availability [9–11], as well as biotic factors, such as competition, facilitation, commensalism, and plant-bacteria interactions. Interactions with plants influence the rhizobacterial community structure by stimulating or repressing bacterial growth [12–14] or by altering the soil microhabitat [4, 15–17]. This influence is mediated, in part, through the release of various compounds into the rhizosphere, which serve as chemical signals or resources for microbial communities [18, 19].

Networks composed of nodes (operational taxon units, OTUs, or amplicon variant sequences, ASVs) and edges (predicted relations among microbes) have been used to explore the ecological interaction patterns among microbial species. Co-occurrence patterns can help to predict “positive or negative interactions” between two microbial taxa, which typically could be interpreted as cooperative or competitive interactions that promote or inhibit growth among them [20–24]. However, there is controversy about the importance of positive and negative interactions in bacterial communities [25], as theoretical and experimental *in vitro* studies indicate that negative interactions are common among bacteria [20, 25–28], while other studies, mainly from natural environments, point to a dominance of positive interactions [10, 16, 24, 29–35], even under nutrient supply conditions [24]. Furthermore, although positive interactions in bacterial communities are expected to promote overall metabolic efficiency [31–33, 36], it has been argued that a prevalence of positive interactions in bacterial communities may decrease community stability because they can lead to metabolic dependencies [20].

Recent investigations have provided clues regarding the role of micronutrients supply in controlling the ecological interactions of bacterial communities [24]. Studies with soil microcosms have indicated that the nutritional status of iron affects the structure of the rhizosphere microbiome [37]. Although iron is abundant in the soil, its availability is often limited because Fe is poorly soluble at neutral and high pH [38–40], especially in the presence of oxygen due to the formation of stable iron oxyhydroxide, hydroxide, and oxides [41, 42]. Recent research also highlighted the influences of iron availability on bacterial interactions and community dynamics in the rhizosphere [43, 44]. At the rhizosphere the formation of soluble

organic chelates is important for iron supply, both plant exudates and secreted bacterial biomolecules that function as chelating agents for metal ions (e.g. siderophores) not only improve the iron mobilization within the soil matrix, alleviating iron deficiency, but also shape the composition and organization of rhizosphere microbial communities [14, 41, 45], suggesting that changes in iron availability represent an opportunity to progress on our knowledge of rhizosphere ecology [46].

In the Atacama Desert, a rich plant diversity can be found in an altitudinal gradient (Talabre-Lejia transect from 2,200 to 4,500 m above sea level) on the western slope of the Andes [47, 48]. The upper limit of this altitudinal transect is dominated by perennial grasses and subshrubs [48], given rise to a patchy distribution of soil properties, with accumulations of plant nutrients under grasses and subshrubs, and leaving arid soils in the inter-plant spaces. Elemental composition analysis indicates that in Talabre-Lejia transect the total Fe content represents between 3 and 5% of the total soil elements present in the soil, while the concentration of soluble Fe varied, in close relation with the soil pH, from 2 to 25 mg kg<sup>-1</sup> [10, 48]. This iron concentration is in the order of magnitude of the Fe concentration found in a study of 32 soil types (3 to 210 mg kg<sup>-1</sup>), which showed that 50 to 90% of the Fe was complexed by organic molecules (i.e., siderophores) suggesting that soil organic matter and its turnover are determining factors for Fe availability in soil.

In this study, we used *Pappostipa frigida*, a native perennial grass as an experimental model [17, 48] and carried out field experiments to alter the nutritional matrix of soil by direct supplementation with iron in two soil compartments: the rhizosphere, where the bacterial community structure is influenced by plant roots, and the surrounding bulk soil. Considering the need of bacteria and plants to satisfy their iron requirements [40, 46], we proposed two hypotheses: (1) the increase in available iron in the soil reduces competition (negative interactions) between bacteria in both soil compartments, rhizosphere, and bulk soil; and (2) the ratio of positive to negative bacterial interactions within the rhizosphere is modulated by the host and responds to iron availability.

## Materials and methods

### Sampling site and experimental design

The study site was located at the steppe region of the Talabre-Lejia transect in the Atacama Desert [48] at 4,370 m above sea level (Fig. 1A). This area is dominated by *Pappostipa frigida* (*P. frigida* (Phil.) Romasch o F. Rojas), a perennial grass, previously described as one of the most abundant plants on the Andes steppe (Fig. 1B) [10]. *P. frigida* develops an important root system that retains an adequate amount of rhizosphere. The experiments were carried out in April 2019, after the

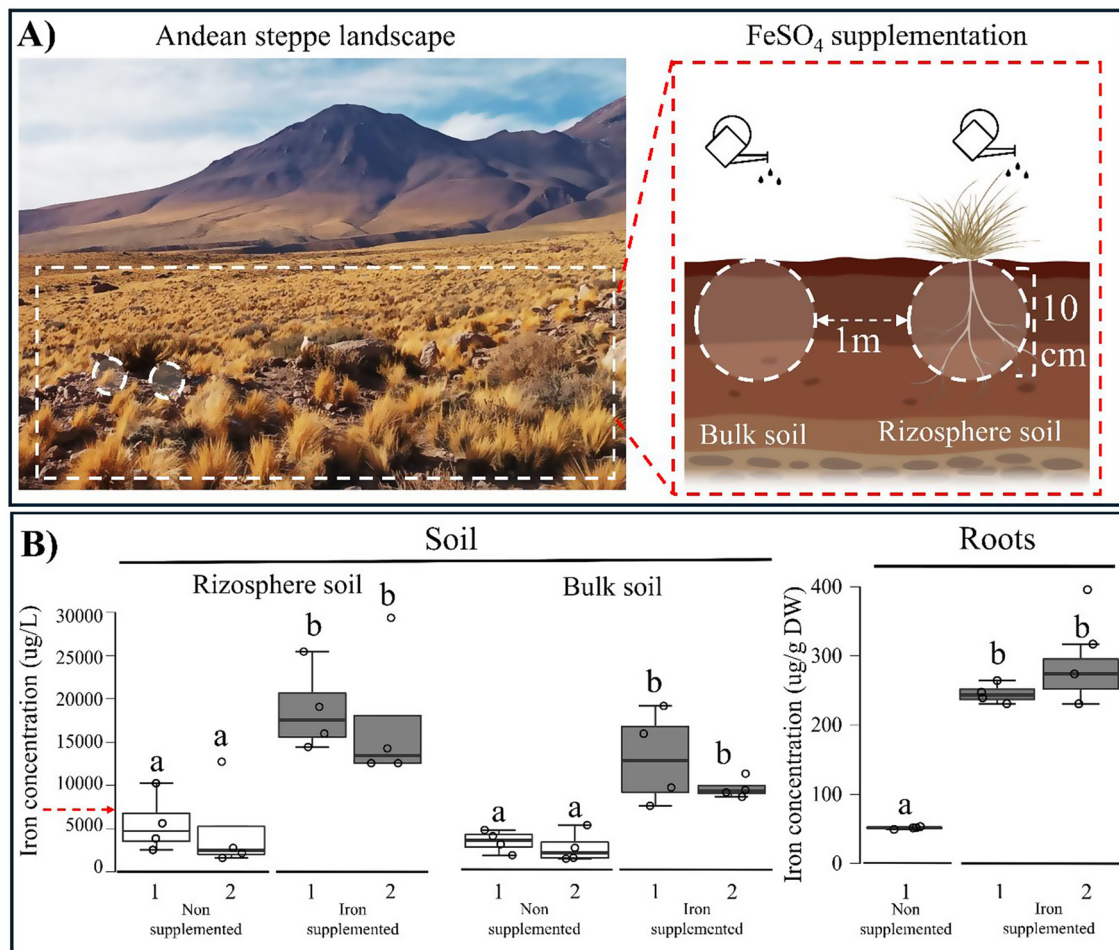


**Fig. 1** Sampling site and experimental strategy. **(A)** Photograph of the study site (10 m<sup>2</sup>), showing an overview of the distribution of the study plant (*Pappostipa frigida*) in the left inset, and the two soil compartments sampled: bulk soil (BS) and rhizosphere soil (RS) in the right inset. **(B)** Box plots of iron concentration in soil samples (µg/L) for non-supplemented samples: 1 (without irrigation) and 2 (irrigated with water) (white boxplots), and iron-supplemented samples: 1 (irrigated with 0.1 mM FeSO<sub>4</sub>) and 2 (irrigated with 0.5 mM FeSO<sub>4</sub>) (grey boxplots). In the right inset, box plots show iron concentration in root samples (µg/g DW). Letters indicate Kruskal-Wallis comparisons ( $p \leq 0.05$ ). The bottom and top of each box represent the 25th and 75th percentiles, the horizontal line within the box is the median, and the ends of the whiskers represent the limits of the distribution, inferred from the upper and lower quartiles. Dots represent individual samples. The red arrow indicates the lowest iron levels reported in agronomic soils (Eshel et al., 2021)

rainy season, which takes place between December and March. We demarcated a 10 m<sup>2</sup> quadrant where randomly selected 16 *P. frigida* plants of equal size that were located on a flat ground, with no plants of other species around. Then, approximately 1 m away from each plant, a point was selected in the bulk soil that lacked plants or roots. Groups of four plants and the corresponding bulk soil of each plant were watered with two liters of solutions of FeSO<sub>4</sub> 0.1 mM or FeSO<sub>4</sub> 0.5 mM, or with two liters of water or left without watering (representing time zero). The solutions and the water were delivered directly to the soil at the base of each plant.

Forty-eight hours after the treatments, we collected 32 soil samples from two different compartments: (1) rhizosphere soil (RS), corresponding to the soil tightly bound to the plant root tissue, and (2) bulk soil (BS).

For each plant, approximately 200 g of RS were recovered as described in [16]. Around 200 g of bulk soil, were obtained at 15 cm deep, after removing the first 2 cm of surface soil. All soil sampling was carried out in sterility, tools were sterilized with ethanol 70% before each collection and the soils, placed in sterile bags, were immediately frozen on dry ice, and transported to the laboratory, where they were stored at -80 °C until DNA extraction. To determine the effect of iron supplementation on iron concentration at soil and root, we collected 10 g of BS and RS and approximately 5 g of plant roots. The samples were stored at 4 °C for Fe, Cu, and Zn content analysis (Table S1).

### Soil classification, physicochemical characteristics and micronutrient properties

Soil order in the sampling area corresponds to Entisols [49]. Soil pH was measured as described by Mandakovic et al. [50]. Soil moisture was monitored using a HOBO U23-001 data logger. The sensor was buried 10 cm deep in unaltered soil at the start of the experiment (time zero) and removed for data collection at the end of the experiment (after 48 h). Soluble Fe, Cu, and Zn contents of BS and RS samples were determined using the total reflection X-ray fluorescence (TXRF) technique [16]. Briefly, 5 g of soil was resuspended in 5 mL of distilled water and homogenized for 2 h at room temperature. After mixing, the samples were centrifuged at 11,440  $\times$  *g* for 10 min in a Hettich Universal 32R centrifuge. The soluble fraction was recovered and used to determine the metal composition. To determine the micronutrient content in root and shoots tissues, the samples were processed and digested as described by del Pozo et al., 2010 [51].

### DNA extraction and 16 S rRNA gene sequencing

Total DNA was extracted from RS and BS soil samples following a previously described protocol [16]. DNA integrity was evaluated by electrophoresis on agarose gel 1% and the DNA was stored at -20 °C until DNA analyses were performed. For each DNA sample ( $N=32$ ), the V1-V3 hypervariable region of the 16 S rDNA gene was amplified using a bacteria-specific primer set: 28 F (5'-GA GTT TGA TCM TGG CTC AG-3') and 519R (5'-GWA TTA CCG CGG CKG CTG-3') [52]. Extraction blanks were included for each DNA extraction to monitor for potential contamination during the extraction process, and no-template controls were used in the amplification to ensure no contamination in the PCR reagents. Sequencing was performed by Mr. DNA (Shallowater, TX, USA) using the Illumina MiSeq platform in an overlapping 2  $\times$  300 bp configuration with a minimum throughput of 51,500 reads per sample. The sequencing outputs were raw sequence data. The Fastq processor application on the website [www.mrdnafreesoftware.com](http://www.mrdnafreesoftware.com) created the file formats expected by QIIME2 for downstream analysis.

### Microbiome bioinformatics analysis

Microbiome bioinformatic analysis was performed using QIIME 2 2021.4 [53]. Raw sequence data were demultiplexed using the q2-demux plugin and quality filter by denoising with DADA2 [54] (via q2-dada2 denoise single). Quality trimming was performed using a Phred score threshold of 30, and primer sequences were trimmed using Cutadapt with a 5% mismatch allowance. Amplicon sequence variants (ASVs) were resolved during the denoising step using DADA2, which uses a denoising algorithm to resolve sequence variants at single

nucleotide resolution, thereby identifying accurate amplicon sequence variants (ASVs). This method avoids arbitrary similarity thresholds (e.g. 97% for OTUs) and allows precise delineation of ASVs. After rarefaction to 51,500 sequences per sample (subsampling without replacement) were taxonomically classified using the QIIME Sklearn method with default parameters [55] against the SILVA r16S database (v.138) [56].

### Microbial diversity analysis

All amplicon sequence variants (ASVs) obtained after denoising were aligned with Mafft (via q2-alignment) and used to construct a phylogeny using fasttree2 [57] (via q2-phylogeny). After rarefaction to 51,500 sequences per sample (subsampling without replacement), microbial alpha diversities were computed with both observed ASVs and Shannon indices using “qiime diversity core-metrics” in QIIME2 plugin.

### Interaction networks based on co-presence and mutual exclusion

Co-occurrence networks were generated using ASV abundance obtained from sequence processing and analysis and visualized using Cytoscape (v3.7.1) [58] with the CoNet plugin [59]. To explore the association with micronutrients, Fe, Cu, and Zn were included in the networks as nodes. ASVs with more than three zero values in the abundance table were eliminated to avoid noise (filter row\_minocc=5). For network construction, two dissimilarity indices (Bray Curtis and Kullback-Leibler) and two correlation indices (Pearson and Spearman) were used to obtain similarity measures. The first threshold was set to generate an initial network containing 500 positive and 500 negative edges, derived from the values obtained for the four similarity measures. The final network was generated using permutation and bootstrapping with 100 iterations. The number of nodes, clustering coefficient, average path length, and density were obtained from the Cytoscape platform. To facilitate the graphical comparison between pairs of networks, without influencing the calculated correlation metrics generated with the CoNet protocol, we used the plot network method implemented in NetCoMi (v1.1.0) [60]. To quantify rewiring in co-occurrence networks between the two conditions (non-supplemented and iron supplemented), we used the Netshift method [61]; this last analysis was carried out as described by Mandakovic et al. [10]. For the analysis of the modules, we selected only those modules with more than ten nodes, which contained approximately 70% of all nodes in the network.

### Statistical analysis

Alpha diversity indices were compared between samples using a pairwise Kruskal-Wallis test, P-values were

corrected using the Benjamini and Hochberg correction method, and false discovery rate (FDR)  $q < 0.05$  was considered statistically significant. Principal coordinate analysis (PCoA) of Bray-Curtis dissimilarity (referred as percentage difference in [62] distance matrices was calculated from count matrix for beta diversity analysis. Permutational (nonparametric) multivariate statistical analysis (perMANOVA) (allowing 999 permutations) was used for group comparisons using MicrobiomeAnalyst [63] (R-based software). Differential abundance analysis between groups of samples was performed using EdgeR [63] at the ASV level using the Stamp [64] platform to compute the test at other taxonomic levels (phylum, order, class, and family) using two-sided Welch's t-test with FDR correction. The relationship between the ASV abundances and the effect of the iron supplementation (iron-supplemented and non-supplemented) and the soil type (rhizosphere and bulk soil) was evaluated using the R package vegan version 2.6-4 [65]. For this analysis, the Hellinger transformation was applied to the count matrix and a transformation-based redundancy analysis (tb-RDA) was performed. The significance of the whole model and the individual axes was tested with a Monte Carlo permutation test (function `anova.cca` of `vegan`). In addition, a transformation-based principal component analysis (tb-PCA) on the transformed data was performed to obtain the maximum variance that could be explained by uncorrelated variables.

## Results

### Effects of iron supplementation on Fe, Cu, and Zn content in soil and roots

To assess the effects of iron supplementation on soils, we conducted a Mann-Whitney test comparing the contents of soluble iron in iron supplemented versus non-supplemented samples. Although 0.1 mM and 0.5 mM supplementation of FeSO<sub>4</sub> caused a significant increase in soil iron content in both the RS and BS compartments, no statistically significant differences between the two iron concentrations were detected (Kruskal-Wallis  $p < 0.05$ ) (Fig. 1A, Table S2). Therefore, in all subsequent analyses, iron supplemented soil samples were referred as iron-supplemented-RS ( $N=8$ ) or iron-supplemented-BS ( $N=8$ ). In addition, the water treatment did not change the iron concentration in soil compared to the soil without watering (Fig. 1A). Regarding soil moisture, our data showed that before treatments, soil relative humidity was above 90%, and no changes were recorded throughout the experimental period of 48-h (Fig. S1). Thus, these samples were referred throughout the text as non-supplemented-RS ( $N=8$ ) or non-supplemented-BS ( $N=8$ ) (Table S1). Nevertheless, all samples ( $N=32$ ) were processed and analyzed separately. Additionally, we assessed the effect of iron supplementation in the concentration of

soluble iron in the roots, and we found that iron supplemented plants had a significantly higher concentration of iron than those of non-supplemented plants (Fig. 1C right panel). When we compare the iron content in the shoots of the non-supplemented plants, which ranged from 250 to 550  $\mu\text{g}/\text{kg}$  DW, with that of the iron-supplemented plants, which ranged from 1600 to 2000  $\mu\text{g}/\text{kg}$  (Table S2.3), we assumed that the iron supplementation has led to an internalization of iron in the plant tissues. Considering previous studies indicating that Zn, Cu and Fe interactions can affect each other absorption and bioavailability by a number of mechanisms [66, 67], as well as, studies showing that excess of one of these metals might alter homeostasis of the others [68], we also examined the effects of iron supplementation on the soluble contents of zinc and copper in soil and roots. We did not find significant changes in the contents of Cu (Fig. S2A) and Zn (Fig. S2B), either in soils or roots of iron-supplemented samples compared with non-supplemented samples, indicating that the iron exposure did not alter the solubility or absorption of the other micronutrients (Kruskal-Wallis  $p > 0.05$ ).

Therefore, the increase in iron concentration in the roots was probably due to plant uptake of the iron supplemented in the soil. Although we acknowledge that the evaluation of the safety of iron supplementation requires toxicological studies to determine the limits of a safe acute exposure, the absence of adverse effects such as signs of chlorosis or size variation in the shoots of *P. frigidula* allowed us to suggest the absence of toxic effects under our experimental condition.

### Taxonomic composition of soil bacterial communities

A total of 22,055 ASVs were identified across all 32 soil samples after rarefaction (51,500 reads) (Table S3). In the rhizosphere, 9,757 ASVs were identified in Non-supplemented-RS samples, and 9,794 in Iron-supplemented-RS samples. In bulk soil, 7,670 ASVs and 8,024 ASVs were identified in Non-supplemented-BS and Iron-supplemented-BS samples, respectively (Fig. S3 and Table S3). The most abundant phyla in rhizosphere samples were Proteobacteria, Acidobacteriota, Bacteroidota, and Actinobacteriota. In bulk soil, Proteobacteria, Actinobacteriota, Chloroflexi, and Acidobacteriota were predominant (Table S3). Approximately 26% of the ASVs were shared between Non-supplemented-RS and Iron-supplemented-RS samples, with a similar trend in bulk soil (Fig. S3). Most ASVs in both rhizosphere and bulk soil were classified as rare (relative abundance  $< 0.1\%$ ) (Table S3). For more details, see supplementary material S1.

### Comparison of bacterial community structure between RS and BS before and after iron-supplementation

Alpha diversity analysis revealed no differences in richness or Shannon index ( $q$ -value  $\leq 0.05$  Kruskal-Wallis test) between non-supplemented and iron supplemented samples neither in RS nor in BS (Fig. 2A and Table S4). To assess whether bacterial community composition differed between the non supplemented and iron supplemented samples, we performed a principal coordinate analysis (PCoA) plot with Bray-Curtis dissimilarity (Fig. 2B). The results also indicated no significant differences between Non-supplemented-RS and Iron-supplemented-RS, nor between Non-supplemented-BS and Iron-supplemented-BS (Fig. 2B).

Nevertheless, the most striking differences were observed between the RS and BS samples (Fig. 3). Thus, the PCoA of the non-supplemented bacterial

communities revealed a significant separation between RS and BS, with PCo1 explaining 53.6% and PCo2 21.4% of the variance (Fig. 3A). Interestingly, differences in beta diversity were lost after iron supplementation ( $q$ -value  $> 0.05$ ) (Fig. 3B). In addition, significant differences in the taxonomic composition between Non-supplemented-RS and Non-supplemented-BS were detected in all taxonomic categories, even at the phylum level (Table S5). For example, 81% of ASVs shared between Non-supplemented-RS and Non-supplemented-BS were differentially abundant (Table S6.1 and Table S6.2), accounting for 40% of the total relative abundance of Non-supplemented-RS samples, whereas only 43% of ASVs shared between Iron-supplemented-RS and Iron-supplemented-BS were differentially abundant, representing 24% of the total relative abundance of Iron-supplemented-RS (Table S6.3 and Table S6.5).

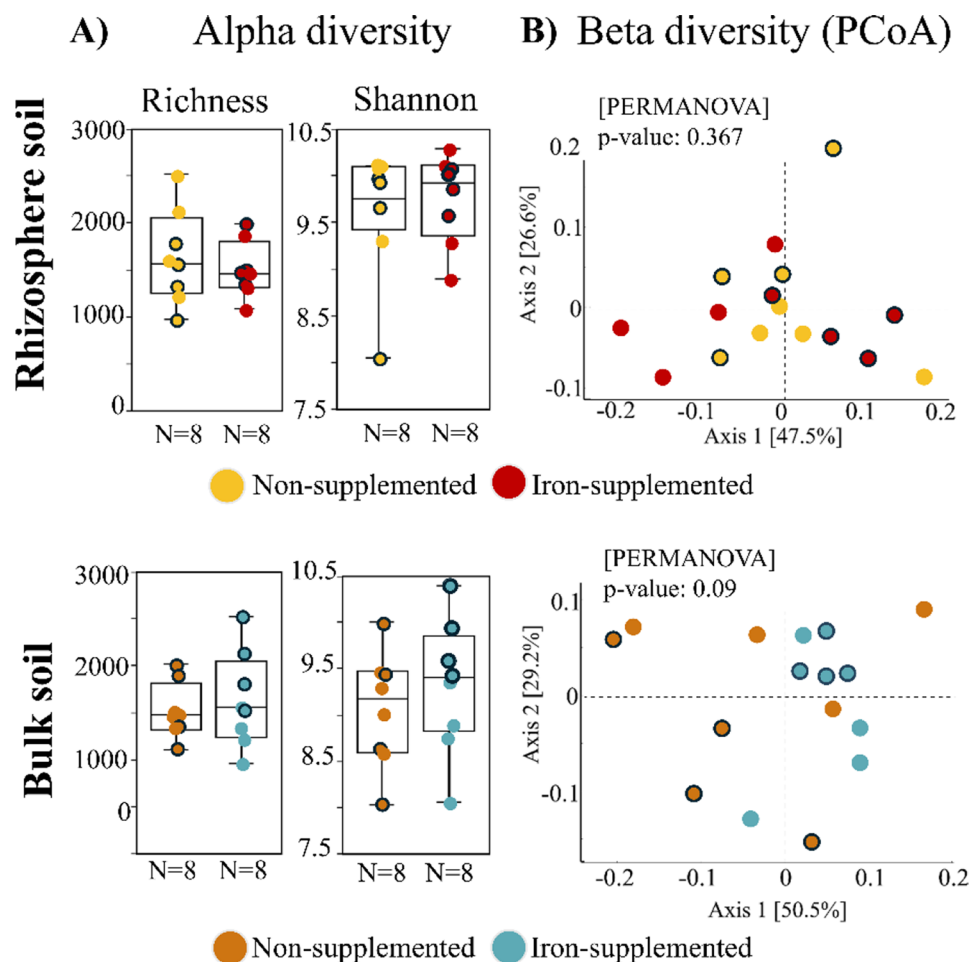


**Fig. 2** Diversity and taxonomic composition between non-supplemented and iron-supplemented samples. **A)** Alpha diversity analysis comparing the non-supplemented samples ( $N=8$ ) and the iron-supplemented samples ( $N=8$ ) in rhizosphere soil and in bulk soil. In both cases, the left panel shows richness calculated with observed\_features index and the right panel alpha diversity calculated with shannon\_index. The bottom and top of a boxed are the 25th and 75th quartiles, the horizontal line within a box is the median, and the ends of the whiskers are the limits of the distribution as inferred from the upper and lower quartiles. Dots are samples. **B)** PcoA plot of Bray-Curtis index between non-supplemented samples ( $N=8$ ) and the iron-supplemented samples ( $N=8$ ) in rhizosphere soil and in bulk soil. Samples irrigated with water or with 0.5 mM FeSO<sub>4</sub> solution are represented with a black border, while samples without water or irrigated with 0.1 mM FeSO<sub>4</sub> solution are without a black border

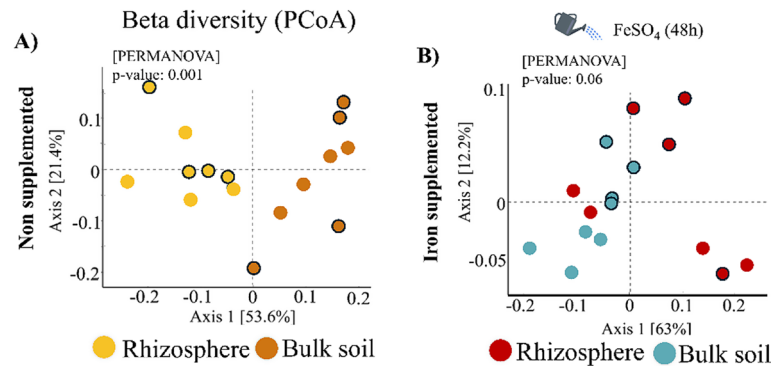


**Fig. 3** Analysis of beta diversity and differential abundance between the rhizosphere and bulk soil samples. PcoA plot of Bray-Curtis index between rhizosphere soil ( $N=8$ ) and bulk soil ( $N=8$ ) non-supplemented samples in **A**) and iron supplemented samples in **B**). Samples irrigated with water or with 0.5 mM  $\text{FeSO}_4$  solution are represented with a black border, while samples without water or irrigated with 0.1 mM  $\text{FeSO}_4$  solution are without a black border

Furthermore, twenty-three families that were differentially abundant between RS and BS without iron supplementation, showed no significant differences after iron exposure (Table S5), including ASVs belonging to families with reported plant growth-promoting effects (Table S6).

To assess the relationship between ASV abundances and the effect of iron supplementation (non-supplemented and iron-supplemented) and soil type (rhizosphere soil and bulk soil), we performed a transformation-based redundancy analysis (tb-RDA) (Fig. S4). The first RDA axis described the soil type, and explains 7.8% of the total variance, while the second RDA axis was related to iron supplementation and explains 4.1%. Both the overall model and the individual axes explain significant variance ( $p\text{-value} < 0.05$ ). In addition, the first two axes of a PCA on the same data set explain 17.8% of the variance. Since this value represents the maximum variance that can be explained by two uncorrelated variables, the first two axes of the RDA (11.9% of the total variance) account for 66.9% of the variance that could be explained by two axes.

#### Effects of iron supplementation on topological parameters of networks

To examine the effect of iron exposure on the co-occurrence patterns in RS and BS bacterial communities, we carried out a quantitative comparison between co-occurrence networks. The number of nodes between non-supplemented and iron supplemented networks was similar in RS (385 and 342 nodes for Non-supplemented-RS and Iron-supplemented-RS networks, respectively) and BS samples (296 and 292 nodes for Non-supplemented-BS and Iron-supplemented-BS networks, respectively) (Fig. 4 and Table S7, S8). Approximately 27% and 21% of the nodes were shared between the iron supplemented and non-supplemented networks generated from the RS and BS samples, respectively (Fig. S5 and Table S7). On the other hand, the number of edges in the rhizosphere

( $n=843$ ) and bulk soil ( $n=721$ ) networks decreased by 30% in both iron supplemented networks (Table S8).

Regarding the ratio between positive and negative interactions, the data showed that this value increased in the iron supplemented networks of both the BS and RS samples. In RS, the ratio increases from 3.2 in Non-supplemented-RS to 4.8 in the Iron-supplemented-RS network, while in BS, the ratio goes from 2.4 in Non-supplemented-BS to 6.8 in the Iron-supplemented-BS network (Fig. 4 and Table S8). To determine whether positive or negative interactions drove the observed increase in the ratio, we compared the types of interactions in the two networks using the Mann-Whitney test. The results showed that negative interactions were significantly decreased in the iron supplemented networks compared to non-supplemented networks in both soil compartments (Fig. S6A).

When the ratio of positive/negative interactions was analyzed considering ASV relative abundance (rare and abundant categories), the following was observed: in the RS compartment, the number of negative interactions decreased in rare nodes (Table S9), mainly between rare interactions (Fig. 4). In the BS compartment, connectivity between abundant nodes showed a generalized decrease (degree, positive degree, and negative degree), whereas connectivity between rare nodes showed a decrease in negative interactions (Table S9). As in RS, in BS, the interactions between rare nodes underwent a more drastic increase in the ratio; although, the ratio of positive/negative interactions increased between rare and abundant nodes (Fig. 4).

#### Comparative analysis of modules in co-occurrence networks

We used the clustering methods from the NetCoMi platform [60], in order to identify groups of nodes that are highly connected to one another but might have few connections to nodes outside their module (Fig. S7 and Table S7). In the RS and BS networks, approximately 90% of all

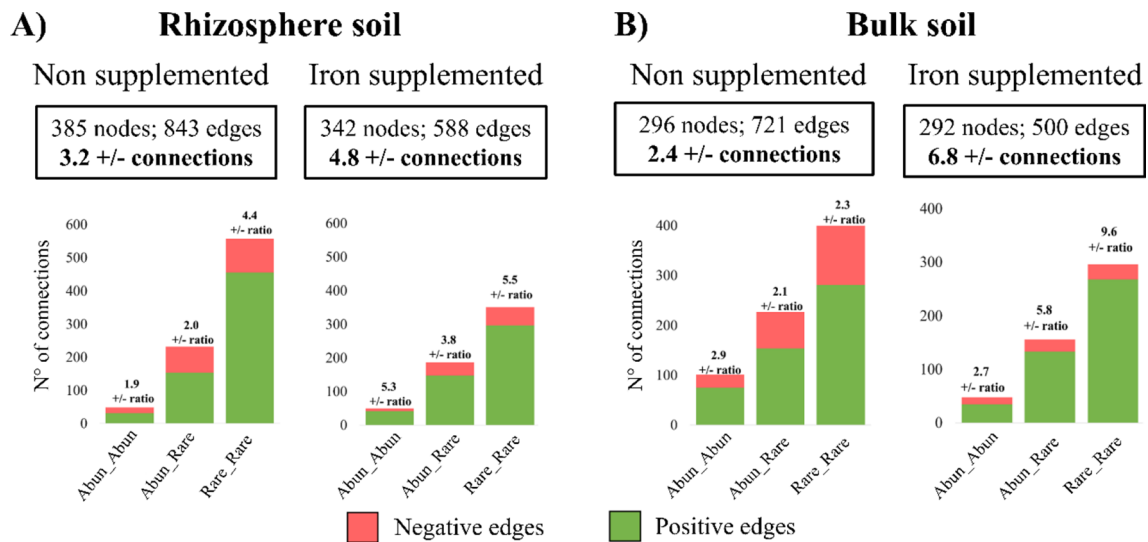


**Fig. 4** Analysis of positive/negative interactions in co-occurrence networks. The figure shows the parameters of the networks (number of nodes, number of edges and ratio between positive and negative interactions) in the upper panel and the bar plots of the analysis of the number of positive and negative interactions between nodes belonging to different abundance categories (abundant-abundant, abundant-rare and rare-rare) in the bottom panel, for the non-supplemented and iron-supplemented networks of rhizosphere networks in **A**) and bulk soil networks in **B**)

positive interactions occurred intra-module, and 70–80% of all negative interactions occurred inter-module (Table S10). In Non-supplemented-RS network, over 40% of the negative interactions occurred between modules I and II, and between modules I and III (Fig. S7A arrows, Table S10). Notably, a node from the Pyrimonadaceae family (belongs Acidobacteriota) in module II had 45 negative interactions with 35 members of module I (Fig. S7A and Tables S7, S10). In the Iron-supplemented-RS network, we did not observe this phenomenon, with only 16 negative interactions between modules IV and V (Fig. S7A, arrows and Table S10). In Non-supplemented-BS, most of 40% of negative interactions occurred between module VI and VII and between VI and VII (Fig. S7B arrows and Table S10). In the Iron-supplemented-BS networks, most of the positive interactions ( $n=92$ ) occurred among the members of module IX, with a notable decrease in the inter-module negative interactions (Table S10).

**Identification of driver taxa in co-occurrence networks**

Using NetShift analysis [61], we identified twenty nodes as candidate drivers in RS and nine in BS (Table S7). To establish the type and number of connections of these nodes, we constructed subnetworks considering only candidate drivers with their respective connections (Fig. 5). When we analyzed the ratio between positive and negative interactions of NetShift nodes in the sub-networks, we observed that in RS the ratio goes from 3.5 to 7.0 (2-fold increase) (Fig. 5A) and in BS from 2.2 to 12.8 (more than 5-fold increase) (Fig. 5B), this drastic increase in the ratio was due to a significant decrease in the negative interactions between members of the

non-supplemented and iron supplemented networks in both RS and BS compartments (Fig S6B). Regarding the relative abundance of twenty candidate drivers detected in Non-supplemented-RS, seven and thirteen candidate driver nodes are abundant and rare respectively, while this number changes to ten and ten in the Iron-supplemented-RS network (Fig. S8 and Table S7). In BS networks, of the nine candidate drivers, seven and two were abundant and rare in the Non-supplemented-BS network and eight and one were abundant and rare after iron supplementation (Fig. S8 and Table S7). Finally, to distinguish between the nodes that interacted with candidate drivers shared or exclusive between non supplemented and iron supplemented networks, we generated Venn diagrams excluding the candidate driver taxa (Fig. S8, lower panel). The results indicated that in the Iron-supplemented-RS network, candidate driver taxa maintained interactions with 16 of the 66 nodes with which they interacted in Non-supplemented-RS network, while in the Iron-supplemented-BS, candidate driver taxa did not maintain any of the connections observed in Non-supplemented-BS. Overall these results suggest a remarkable remodeling of soil bacterial community after iron supplementation (Fig. S8).

**Discussion**

**Iron supplementation influences beta-diversity of soil bacterial communities**

Understanding how soil bacterial communities respond to environmental changes, such as nutrient availability, is crucial to address global challenges like desertification and climate change [69]. Soil microorganisms in the

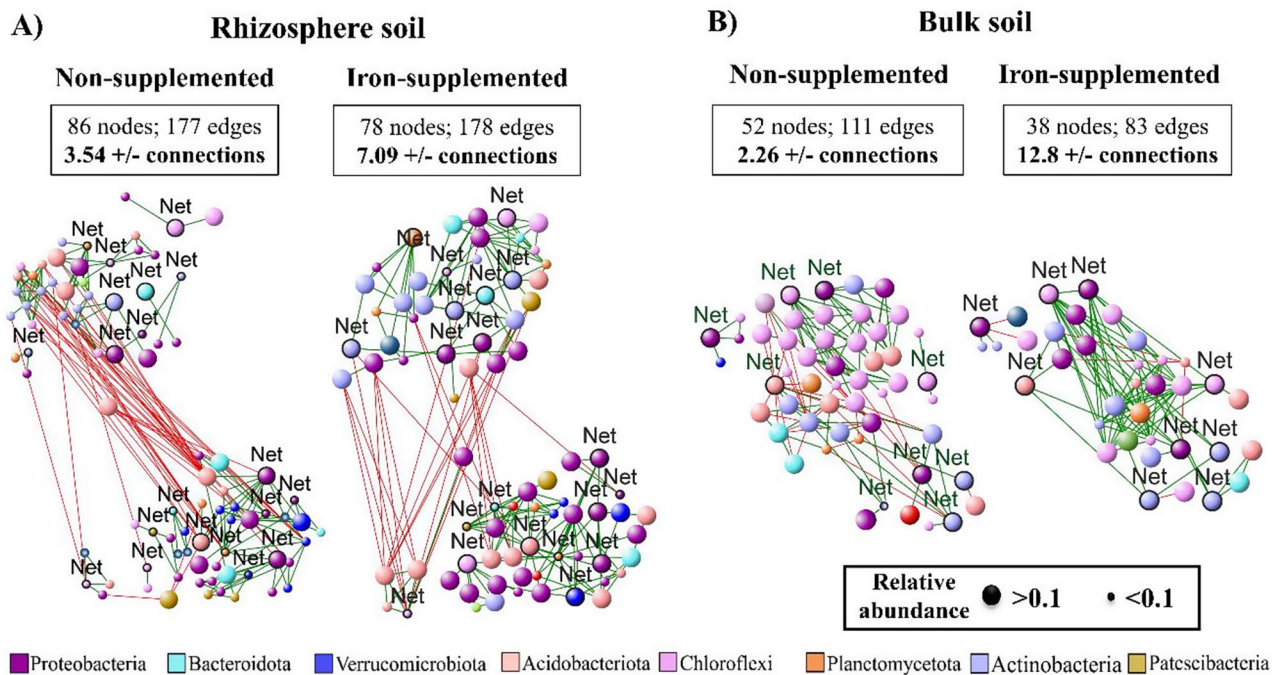


**Fig. 5** Candidate driver co-occurrence networks of non-supplemented and iron-supplemented samples in the rhizosphere and bulk soil. Co-occurrence networks were constructed using only candidate driver nodes and the nodes to which they are connected in non-supplemented and iron-supplemented samples of rhizosphere soil **A)** and bulk soil **B)**. Interactions were inferred from bacterial ASVs abundances. Each node represents ASVs annotated at the phylum level and edges represent positive (co-occurrence) or negative (exclusion) correlations between the relative abundances of the ASVs. Finally, the size of the nodes indicates whether the ASVs belong to abundant (relative abundance >0.1) or rare (relative abundance <0.1) abundance categories. Candidate driver nodes are identified by the word “Net”

Andes of Atacama Desert cope with a general nutrient limitation, including a low availability of soluble iron [48, 70], a metal that has a predominant role in microorganism communities [71]. In this work, compared to reference values [48], the soluble iron content in the BS and RS compartments was below the lower limit detected in agronomic soils. After iron supplementation, the soluble content of the metal increased, reaching a value that exceeded 1.4 to 1.9 times the minimal agricultural reference value for this nutrient. Moreover, after iron supplementation, the iron content in the root tissue of *P. frigida* increased four to five times, suggesting that *P. frigida* root system was able to absorb the supplemented iron and that the plant was far from its maximum iron storage capacity. Thus, it seems reasonable to assume that changes in the structure and interaction pattern of the bacterial community were associated with an increase in iron availability due to iron supplementation in the soil.

Surprisingly, beta-diversity analysis revealed that before supplementation, the BS and RS bacterial communities of *P. frigida* showed marked dissimilarity and after supplementation, this dissimilarity no longer persisted. Interestingly, an increase in beta diversity or community dispersion has been observed across different environments and stressor types [72]. In this scenario, the observed changes in beta diversity could be interpreted

according to the Anna Karenina principle [73], i.e. “stressed microbiota vary more than those unstressed” [74]. In this line of reasoning, Rocca et al. [72] suggests that stress increases beta diversity (dissimilarity) among microbial communities, and when stress decreases, the differences in beta diversity caused by the stressor also decreases, making the communities more similar to each other. Thus, our results indicate that iron availability can be a crucial factor driving microbiome structure and assembly in both the BS and the RS. Although plant species tend to assemble relatively distinct rhizobacterial communities [74] by stimulating or repressing bacterial growth [12–14] or by altering the soil microhabitat [15–17], Our results suggest that the increase in iron content produced by supplementation modified the availability of iron in BS and RS, shaping the assembly of microbiomes in both compartments. On the other hand, it is known that the nutrient status of the plant has a profound effect on the exudation pattern of the roots [38, 75], therefore it the increment of iron in roots of *P. frigida* may have triggered a response in the plant, affecting the plant–microbe interactions at the rhizosphere level. In fact, the rhizosphere of *P. frigida* exhibits a variety of compounds such as organic acids, sugars, as well as, primary and secondary metabolites [18] that might have a substantial influence on the composition and structure of the rhizosphere

microbiome [19, 41]. In this context, the synthesis of plant-derived coumarin in response to changes in iron availability has been shown to modulate the composition of rhizosphere [38, 43, 76] due to coumarin antimicrobial activity [43]. Interestingly, among the wide range of metabolites that *P. frigida* exudes, the presence of coumarins was detected [18]. Thus, we speculate that synthesis and secretion of coumarin (without iron supplementation), may be part of the mechanism that sustains the dissimilarity between BS and RS of *P. frigida*, a mechanism that could be altered after iron supplementation. However, further studies are required to evaluate when coumarin synthesis and secretion decreases in response to an increase in iron availability.

In terms of how the change in beta diversity metrics was produced, our data indicate that the percentage of ASVs with significant differences in abundance between BS and RS decreased from 81 to 43% after iron supplementation, including known plant growth-promoting bacteria [48]. At the family level, 23 families representing the 17% of relative abundance in RS, exhibited significant differences in their relative abundance only before iron supplementation. This result supports the notion that the recruitment strategy of plants can be modulated by the nutrient availability, as has been proposed by Trivedi et al. [77] for plants under iron or phosphorus stress conditions.

Moreover, iron availability can modify the ecological interactions among members of the bacterial community. For example, it has been suggested that the low availability of iron in soil and the high iron demand of plants and microorganisms could induce a considerable level of competition for iron in the rhizosphere [78, 79].

#### **Iron modifies the positive/negative interactions in soil bacterial communities**

Since that the ratio of positive/negative interactions strongly impacts the structure of the bacterial communities [20, 80], we assessed whether iron supplementation modulates the ratio of positive/negative interactions in the BS and RS bacterial communities. Our results showed that most of the negative interactions were inter-modules while positive interactions were intra-modules and that according to our hypothesis, negative interactions decreased among members of bacterial communities both in the BS and RS compartments after iron supplementation, mainly among rare taxa. The decrease in negative interactions in response to iron was also observed in the subnetworks of candidate driver taxa. Interestingly, two of the three driver taxa that change their abundance from rare to abundant after iron supplementation belong to the genera *Blastococcus* (Actinobacteria) and *Haliangium* (Proteobacteria), which are more abundant in the bulk soil than the rhizosphere [80] suggesting that these

bacteria respond to change of iron availability increasing their abundance and modifying the interaction pattern of bacterial community. The third driver taxa belong to *Sphingomonadaceae* family (Proteobacteria), which has been observed to enhance plant growth [81], suggesting that these bacteria could connect the function of PGP with the assembly of bacterial community.

As observed within the microbiomes of diverse plant hosts [82, 83], the rhizosphere of *P. frigida* showed a large proportion of low abundance species (relative abundance less than 0.1% or 0.01%) defined as “rare biosphere” [28, 84], which may be the result of competition induced by nutrient-poor conditions [83]. It is therefore reasonable to assume that an increase in iron concentration will reduce the competition for this micronutrient, especially in rare taxa. This idea is supported by a study comparing bacterial communities in nutrient-rich coastal sediment and nutrient-scarce pelagic zones of the ocean [24], and demonstrates that the abundance profiles of bacterial species (rare versus abundant) were influenced by nutrient availability. Furthermore, a continental-scale study in the eastern China [85] showed that the factors that most affected co-occurrence relationships between taxa were organic matter and iron content, further supporting the importance of these factors on soil bacterial interactions.

On the other hand, co-occurrence networks showed that there was a 3-fold increase in the ratio of positive/negative interactions within bulk soil bacterial community, while in the *P. frigida* rhizosphere the increase was 1.5-fold. Since cooperative interactions in bacterial communities promote overall metabolic efficiency [86], an increase in positive interactions may be beneficial to the community. However, an increase in cooperativity can result in a decrease in bacterial community stability, as it may lead to metabolic dependencies among bacteria [20]. Considering that bacterial communities not only evolve, but also co-evolve with their host [86], it is of vital importance for the host, as well as for any taxa being part of their associated microbiome, that the community equilibrium remains stable. Following this line of reasoning, our results provide empirical evidence in support to the model of Coyte et al. [20], which proposes that the host can impose a limitation to increase cooperativity (in our case caused by iron availability) within the community. In a more practical context, this study contributes to understanding the effects of nutrient supplementation strategies on microbial interactions and their impact on plant health, a knowledge that will help to develop nutritional interventions in arid regions.

#### **Study limitations and perspectives**

Although valuable insights were gained in this study by applying an experimental strategy to test ecological theories in a natural environment, some limitations need

to be considered. First, the length of the experimental intervention, the use of a single iron pulse, and the short interval between its application and sampling may not have been enough to capture the full extent of microbial community responses to iron supplementation over time. For example, it has been proposed that the Anna Karenina principle may be a transient state in nature that may precede the resilience of the animal/plant holobiont [74]. Alternatively, the loss of dissimilarity in microbiome composition between bulk and rhizosphere soils could be a consequence of the selection pressure exerted by the iron supplementation on the microbiome and/or plant, overcoming or masking the differentiating effect exerted by the plant exudates. When the effect of iron supplementation dissipates, we can expect that differences in beta diversity between BS and RS will be restored. Second, it is important to be cautious when interpreting interactions between taxa predicted by co-occurrence network analysis, as they are often interpreted as direct biotic interactions (true ecological relationships such as competition or cross-feeding). However, they may reflect changes in indirect interactions among species that correlate as a consequence of responding in the same way to iron supplementation.

## Conclusions

Our study indicates that iron supplementation led to a significant reduction in the beta diversity difference between rhizosphere soil and bulk soil, suggesting that iron has a role in the differentiation between these two compartments. Additionally, the co-occurrence networks revealed a notable decrease in negative interactions among soil bacteria, particularly among rare taxa. These findings suggest that changes of iron availability play an important role in shaping the bacterial community dynamics, enhancing cooperation while reducing competition. Although, the distinct effect of iron supplementation in competition/cooperation ratio between the rhizosphere and bulk soil supports the notion that the host plant modulates the degree of cooperation that can be reached by a bacterial community associated with a host.

## Supplementary Information

The online version contains supplementary material available at <https://doi.org/10.1186/s40793-024-00661-7>.

Supplementary Material 1  
Supplementary Material 2  
Supplementary Material 3  
Supplementary Material 4

## Acknowledgements

We thank Dr. Marco Pfeiffer for very helpful assistance with soil classification data and to our two anonymous reviewers for their constructive comments. The authors would like to thank Comunidad Talabre, Antofagasta, Chile, for granted access to the TLT sampling zone.

## Author contributions

M.G.: Conceptualization, Investigation, Formal analysis, Writing of the original draft, Writing review & editing. C.A-N.: Conceptualization, Investigation, Methodology, Formal analysis, Writing of the original draft, Writing review & editing. J.M.: Conceptualization, methodology, Writing review & editing. G.G.: Formal analysis. Daniel E. Palma: Formal analysis. C.H.: Formal analysis, Writing review & editing. V.C.: Conceptualization, Investigation, Formal analysis, Writing review & editing. All authors reviewed the manuscript.

## Funding

This study was funded by ANID FONDECYT grants 1201278, 1241424 to MG and 1211893 to VC, Millennium Science Initiative Program: ICN2021\_044 and ANID/SIA SA77210103 to JM.

## Data availability

Sequences are available at NCBI public repository under the BioProject accession number PRJNA1102656. The code used for data analysis is available in the following link <https://github.com/CotyAguado/Ironing-the-conflicts/blob/main/Code>. In addition, a Jupyter notebook containing the code used to generate the network layouts with NetCoMi is available in the following link <https://github.com/CotyAguado/Ironing-the-conflicts/blob/main/networks.ipynb>.

## Declarations

### Ethics approval and consent to participate

Not applicable.

### Consent for publication

Not applicable.

### Competing interests

The authors declare no competing interests.

Received: 30 August 2024 / Accepted: 22 December 2024

Published online: 11 March 2025

## References

1. Thompson LR, Sanders JG, McDonald D, Amir A, Ladau J, Locey KJ, et al. A communal catalogue reveals Earth's multiscale microbial diversity. *Nature*. 2017;551:457–63.
2. Bahram M, Hildebrand F, Forslund SK, Anderson JL, Soudzilovskaia NA, Bodegom PM, et al. Structure and function of the global topsoil Microbiome. *Nature*. 2018;560:233–7.
3. Jones SE, Lennon JT. Dormancy contributes to the maintenance of microbial diversity. *Proceedings of the National Academy of Sciences*. 2010;107:5881–6.
4. Fierer N, Jackson RB. The diversity and biogeography of soil bacterial communities. *Proceedings of the National Academy of Sciences*. 2006;103:626–31.
5. Lauber CL, Hamady M, Knight R, Fierer N. Pyrosequencing-Based assessment of soil pH as a predictor of soil bacterial community structure at the continental scale. *Appl Environ Microbiol*. 2009;75:5111–20.
6. Angel R, Soares MIM, Ungar ED, Gillor O. Biogeography of soil archaea and bacteria along a steep precipitation gradient. *ISME J*. 2010;4:553–63.
7. Neilson JW, Califf K, Cardona C, Copeland A, van Treuren W, Josephson KL, et al. Significant impacts of increasing aridity on the arid soil Microbiome. *mSystems*. 2017;2. <https://doi.org/10.1128/mSystems.00195-16>.
8. Stomeo F, Makhalanyane TP, Valverde A, Pointing SB, Stevens MI, Cary CS, et al. Abiotic factors influence microbial diversity in permanently cold soil horizons of a maritime-associated Antarctic dry Valley. *FEMS Microbiol Ecol*. 2012;82:326–40.
9. Li F, Chen L, Zhang J, Yin J, Huang S. Bacterial community structure after Long-term organic and inorganic fertilization reveals important associations

- between soil nutrients and specific taxa involved in nutrient transformations. *Front Microbiol.* 2017;8.
10. Mandakovic D, Rojas C, Maldonado J, Latorre M, Travisany D, Delage E, et al. Structure and co-occurrence patterns in microbial communities under acute environmental stress reveal ecological factors fostering resilience. *Sci Rep.* 2018;8:5875.
  11. Kalwani M, Chakdar H, Srivastava A, Pabbi S, Shukla P. Effects of nanofertilizers on soil and plant-associated microbial communities: emerging trends and perspectives. *Chemosphere.* 2022;287:132107.
  12. Bais HP, Weir TL, Perry LG, Gilroy S, Vivanco JM. The role of root exudates in rhizosphere interactions with plants and other organisms. *Annual Review of Plant Biology.* 2006;57:233–66.
  13. Doornbos RF, van Loon LC, Bakker PAHM. Impact of root exudates and plant defense signaling on bacterial communities in the rhizosphere. A review. *Agron Sustain Dev.* 2012;32:227–43.
  14. Sasse J, Martinoia E, Northen T. Feed your friends: do plant exudates shape the root microbiome? *Trends Plant Sci.* 2018;23:25–41.
  15. Berendsen RL, Pieterse CMJ, Bakker PAHM. The rhizosphere Microbiome and plant health. *Trends Plant Sci.* 2012;17:478–86.
  16. Mandakovic D, Aguado-Norese C, García-Jiménez B, Hodar C, Maldonado JE, Gaete A, et al. Testing the stress gradient hypothesis in soil bacterial communities associated with vegetation belts in the Andean Atacama desert. *Environ Microbiome.* 2023;18:24.
  17. Fernández-Gómez B, Maldonado J, Mandakovic D, Gaete A, Gutiérrez RA, Maass A, et al. Bacterial communities associated to Chilean altiplanic native plants from the Andean grasslands soils. *Sci Rep.* 2019;9:1042.
  18. Dussarrat T, Latorre C, Barros Santos MC, Aguado-Norese C, Prigent S, Díaz FP, et al. Rhizochemistry and soil bacterial community are tailored to natural stress gradients. *Soil Biol Biochem.* 2025;202:109662.
  19. Solomon W, Janda T, Molnár Z. Unveiling the significance of rhizosphere: implications for plant growth, stress response, and sustainable agriculture. *Plant Physiol Biochem.* 2024;206:108290.
  20. Coyte KZ, Schluter J, Foster KR. The ecology of the microbiome: networks, competition, and stability. *Science.* 2015;350:663–6.
  21. Dundore-Arias JP, Michalska-Smith M, Millican M, Kinkel LL. More Than the Sum of Its Parts: Unlocking the Power of Network Structure for Understanding Organization and Function in Microbiomes. *Annual Review of Phytopathology.* 2023;61:403–23.
  22. Faust K, Raes J. Microbial interactions: from networks to models. *Nat Rev Microbiol.* 2012;10:538–50.
  23. Koder SM, Das P, Gilbert JA, Lutz HL. Conceptual strategies for characterizing interactions in microbial communities. *iScience.* 2022;25:103775.
  24. Dai T, Wen D, Bates CT, Wu L, Guo X, Liu S, et al. Nutrient supply controls the linkage between species abundance and ecological interactions in marine bacterial communities. *Nat Commun.* 2022;13:175.
  25. Palmer JD, Foster KR. Bacterial species rarely work together. *Science.* 2022;376:581–2.
  26. Baichman-Kass A, Song T, Friedman J. Competitive interactions between culturable bacteria are highly non-additive. *eLife.* 2023;12:e83398.
  27. Foster KR, Bell T. Competition Not cooperation, dominates interactions among culturable microbial species. *Curr Biol.* 2012;22:1845–50.
  28. Kurm V, van der Putten WH, Weidner S, Geisen S, Snoek BL, Bakx T, et al. Competition and predation as possible causes of bacterial rarity. *Environ Microbiol.* 2019;21:1356–68.
  29. Kehe J, Ortiz A, Kulesa A, Gore J, Blainey PC, Friedman J. Positive interactions are common among culturable bacteria. *Sci Adv.* 2021;7:eabi7159.
  30. Blasche S, Kim Y, Mars RAT, Machado D, Maansson M, Kafkia E, et al. Metabolic Cooperation and Spatiotemporal niche partitioning in a Kefir microbial community. *Nat Microbiol.* 2021;6:196–208.
  31. Calatayud J, Andivia E, Escudero A, Melián CJ, Bernardo-Madrid R, Stoffel M, et al. Positive associations among rare species and their persistence in ecological assemblages. *Nat Ecol Evol.* 2020;4:40–5.
  32. Shi S, Nuccio EE, Shi ZJ, He Z, Zhou J, Firestone MK. The interconnected rhizosphere: high network complexity dominates rhizosphere assemblages. *Ecol Lett.* 2016;19:926–36.
  33. Luo J, Guo X, Tao Q, Li J, Liu Y, Du Y, et al. Succession of the composition and co-occurrence networks of rhizosphere microbiota is linked to Cd/Zn hyperaccumulation. *Soil Biol Biochem.* 2021;153:108120.
  34. Xing W, Gai X, Ju F, Chen G. Microbial communities in tree root-compartment niches under Cd and Zn pollution: structure, assembly process and co-occurrence relationship. *Sci Total Environ.* 2023;860:160273.
  35. Maldonado JE, Gaete A, Mandakovic D, Aguado-Norese C, Aguilar M, Gutiérrez RA, et al. Partners to survive: Hoffmannseggia doellii root-associated Microbiome at the Atacama desert. *New Phytol.* 2022;234:2126–39.
  36. García-Bayona L, Comstock LE. Bacterial antagonism in host-associated microbial communities. *Science.* 2018;361:eaat2456.
  37. Yang C-H, Crowley DE. Rhizosphere microbial community structure in relation to root location and plant Iron nutritional status. *Appl Environ Microbiol.* 2000;66:345–51.
  38. Stassen MJJ, Hsu S-H, Pieterse CMJ, Stringlis IA. Coumarin communication along the Microbiome–Root–Shoot Axis. *Trends Plant Sci.* 2021;26:169–83.
  39. Schmidt W. Iron solutions: acquisition strategies and signaling pathways in plants. *Trends Plant Sci.* 2003;8:188–93.
  40. Colombo C, Palumbo G, He J-Z, Pinton R, Cesco S. Review on iron availability in soil: interaction of Fe minerals, plants, and microbes. *J Soils Sediments.* 2014;14:538–48.
  41. Molnár Z, Solomon W, Mutum L, Janda T. Understanding the mechanisms of Fe deficiency in the rhizosphere to promote plant resilience. *Plants.* 2023;12:1945.
  42. Vélez-Bermúdez IC, Schmidt W. Plant strategies to mine iron from alkaline substrates. *Plant Soil.* 2023;483:1–25.
  43. Voges MJEE, Bai Y, Schulze-Lefert P, Sattely ES. Plant-derived coumarins shape the composition of an Arabidopsis synthetic root microbiome. *Proceedings of the National Academy of Sciences.* 2019;116:12558–65.
  44. Zhang C, Liu S, Hussain S, Li L, Baiome BA, Xiao S, et al. Fe(II) addition drives soil bacterial Co-Occurrence patterns and functions mediated by anaerobic and chemoautotrophic taxa. *Microorganisms.* 2022;10:547.
  45. Dai Z, Guo X, Lin J, Wang X, He D, Zeng R, et al. Metallic micronutrients are associated with the structure and function of the soil Microbiome. *Nat Commun.* 2023;14:8456.
  46. Lemanceau P, Bauer P, Kraemer S, Briat J-F. Iron dynamics in the rhizosphere as a case study for analyzing interactions between soils, plants and microbes. *Plant Soil.* 2009;321:513–35.
  47. Carrasco-Puga G, Díaz FP, Soto DC, Hernández-Castro C, Contreras-López O, Maldonado A, et al. Revealing hidden plant diversity in arid environments. *Ecography.* 2021;44:98–111.
  48. Eshel G, Arous V, Undurraga S, Soto DC, Moraga C, Montecinos A, et al. Plant ecological genomics at the limits of life in the Atacama Desert. *Proceedings of the National Academy of Sciences.* 2021;118:e2101177118.
  49. Casanova M, Salazar O, Seguel O, Luzzio W. The soils of Chile. Dordrecht: Springer Netherlands; 2013.
  50. Mandakovic D, Maldonado J, Pulgar R, Cabrera P, Gaete A, Urtuvia V, et al. Microbiome analysis and bacterial isolation from Lejía lake soil in Atacama desert. *Extremophiles.* 2018;22:665–73.
  51. del Pozo T, Cambiazo V, González M. Gene expression profiling analysis of copper homeostasis in Arabidopsis thaliana. *Biochem Biophys Res Commun.* 2010;393:248–52.
  52. Turner S, Pryer KM, Miao VPW, Palmer JD. Investigating deep phylogenetic relationships among Cyanobacteria and plastids by small subunit rRNA sequence Analysis 1. *J Eukaryot Microbiol.* 1999;46:327–38.
  53. Bolyen E, Rideout JR, Dillon MR, Bokulich NA, Abnet CC, Al-Ghalith GA, et al. Reproducible, interactive, scalable and extensible Microbiome data science using QIIME 2. *Nat Biotechnol.* 2019;37:852–7.
  54. Callahan BJ, McMurdie PJ, Rosen MJ, Han AW, Johnson AJA, Holmes SP. DADA2: High-resolution sample inference from illumina amplicon data. *Nat Methods.* 2016;13:581–3.
  55. Pedregosa F, Varoquaux G, Gramfort A, Michel V, Thirion B, Grisel O, et al. Scikit-learn: machine learning in Python. *MACHINE LEARNING IN PYTHON.*
  56. Quast C, Pruesse E, Yilmaz P, Gerken J, Schweer T, Yarza P, et al. The SILVA ribosomal RNA gene database project: improved data processing and web-based tools. *Nucleic Acids Res.* 2013;41:D590–6.
  57. Katoh K, Misawa K, Kuma K, Miyata T. MAFFT: a novel method for rapid multiple sequence alignment based on fast fourier transform. *Nucleic Acids Res.* 2002;30:3059–66.
  58. Shannon P, Markiel A, Ozier O, Baliga NS, Wang JT, Ramage D, et al. Cytoscape: A software environment for integrated models of biomolecular interaction networks. *Genome Res.* 2003;13:2498–504.
  59. Faust K, Raes J. CoNet app: inference of biological association networks using cytoscape. *F1000Res.* 2016;5:1519.
  60. Peschel S, Müller CL, von Mutius E, Boulesteix A-L, Depner M. NetCoMi: network construction and comparison for Microbiome data in R. *Brief Bioinform.* 2021;22:bbaa290.

61. Kuntal BK, Chandrakar P, Sadhu S, Mande SS. NetShift': a methodology for Understanding 'driver microbes' from healthy and disease Microbiome datasets. *ISME J.* 2019;13:442–54.
62. Legendre P, Legendre L. Numerical ecology. Elsevier; 2012.
63. Lu Y, Zhou G, Ewald J, Pang Z, Shiri T, Xia J. MicrobiomeAnalyst 2.0: comprehensive statistical, functional and integrative analysis of Microbiome data. *Nucleic Acids Res.* 2023;51:W310–8.
64. Parks DH, Tyson GW, Hugenholtz P, Beiko RG. STAMP: statistical analysis of taxonomic and functional profiles. *Bioinformatics.* 2014;30:3123–4.
65. Oksanen J, Simpson G, Blanchet F, Kindt R, Legendre P, Minchin P, et al. vegan: Community Ecology Package. R package version 2.6–4. 2022. 2023.
66. Arredondo M, Núñez MT. Iron and copper metabolism. *Mol Aspects Med.* 2005;26:313–27.
67. Espinoza A, Le Blanc S, Olivares M, Pizarro F, Ruz M, Arredondo M. Iron, copper, and zinc transport: Inhibition of divalent metal transporter 1 (DMT1) and human copper transporter 1 (hCTR1) by ShRNA. *Biol Trace Elem Res.* 2012;146:281–6.
68. Xu Z, Wang P, Wang H, Yu ZH, Au-Yeung HY, Hirayama T, et al. Zinc excess increases cellular demand for iron and decreases tolerance to copper in *Escherichia coli*. *J Biol Chem.* 2019;294:16978–91.
69. Osborne P, Hall LJ, Kronfeld-Schor N, Thybert D, Haerty W. A rather dry subject; investigating the study of arid-associated microbial communities. *Environ Microbiome.* 2020;15:20.
70. Soussi A, Ferjani R, Marasco R, Guesmi A, Cherif H, Rolli E, et al. Plant-associated microbiomes in arid lands: diversity, ecology and biotechnological potential. *Plant Soil.* 2016;405:357–70.
71. Andrews SC, Robinson AK, Rodríguez-Quiriones F. Bacterial iron homeostasis. *FEMS Microbiol Rev.* 2003;27:215–37.
72. Rocca JD, Simonin M, Blaszcak JR, Ernakovich JG, Gibbons SM, Midani FS, et al. The Microbiome stress project: toward a global Meta-Analysis of environmental stressors and their effects on microbial communities. *Front Microbiol.* 2019;9.
73. Zaneveld JR, McMinds R, Vega Thurber R. Stress and stability: applying the Anna karenina principle to animal microbiomes. *Nat Microbiol.* 2017;2:1–8.
74. Arnault G, Mony C, Vandenkoornhuyse P. Plant microbiota dysbiosis and the Anna karenina principle. *Trends Plant Sci.* 2023;28:18–30.
75. Carvalhais LC, Dennis PG, Fedoseyenko D, Hajirezaei M-R, Borriss R, von Wirén N. Root exudation of sugars, amino acids, and organic acids by maize as affected by nitrogen, phosphorus, potassium, and iron deficiency. *J Plant Nutr Soil Sci.* 2011;174:3–11.
76. Murgia I, Marzorati F, Vigani G, Morandini P. Plant iron nutrition: the long road from soil to seeds. *J Exp Bot.* 2022;73:1809–24.
77. Trivedi P, Leach JE, Tringe SG, Sa T, Singh BK. Plant–microbiome interactions: from community assembly to plant health. *Nat Rev Microbiol.* 2020;18:607–21.
78. Contreras-Moreno FJ, Moraleda-Muñoz A, Marcos-Torres FJ, Cuéllar V, Soto MJ, Pérez J, et al. Siderophores and competition for iron govern myxobacterial predation dynamics. *ISME J.* 2024;18:wrae077.
79. Guerinot ML, Yi Y. Iron Nutritious, noxious, and not readily available. *Plant Physiol.* 1994;104:815–20.
80. Ling N, Wang T, Kuzyakov Y. Rhizosphere bacteriome structure and functions. *Nat Commun.* 2022;13:836.
81. Asaf S, Numan M, Khan AL, Al-Harrasi A. Sphingomonas: from diversity and genomics to functional role in environmental remediation and plant growth. *Crit Rev Biotechnol.* 2020;40:138–52.
82. Sogin ML, Morrison HG, Huber JA, Welch DM, Huse SM, Neal PR, et al. Microbial diversity in the deep sea and the underexplored rare biosphere. *Proceedings of the National Academy of Sciences.* 2006;103:12115–20.
83. Jousset A, Bienhold C, Chatzinotas A, Gallien L, Gobet A, Kurm V, et al. Where less May be more: how the rare biosphere pulls ecosystems strings. *ISME J.* 2017;11:853–62.
84. Guseva K, Darcy S, Simon E, Alteio LV, Montesinos-Navarro A, Kaiser C. From diversity to complexity: microbial networks in soils. *Soil Biol Biochem.* 2022;169:108604.
85. Ma B, Wang Y, Ye S, Liu S, Stirling E, Gilbert JA, et al. Earth microbial co-occurrence network reveals interconnection pattern across microbiomes. *Microbiome.* 2020;8:82.
86. Rosenberg E, Zilber-Rosenberg I. Microbes drive evolution of animals and plants: the hologenome concept. *mBio.* 2016;7. <https://doi.org/10.1128/mbio.01395-15>.

## Publisher's note

Springer Nature remains neutral with regard to jurisdictional claims in published maps and institutional affiliations.